2013

Fluidization Assistance of Nanopowders by an Alternating Nonuniform Electric Field

M.A.S. Quintanilla
University of Seville, Spain

J. M. Valverde
University of Seville, Spain

M. J. Espin
University of Seville, Spain

FLUIDIZATION ASSISTANCE OF NANOPOWDERS BY AN ALTERNATING NONUNIFORM ELECTRIC FIELD

M.A.S. Quintanilla[a], J. M. Valverde[a]*, M. J. Espin[b],
University of Seville; [a]Dept. Electronics and Electromagnetism; [b]Dept. Applied Physics II;; Avda. Reina Mercedes s/n, 41012 Seville, Spain
*T: +34-954550960; F: +34-954239434; E: jmillan@us.es

ABSTRACT
Usually, nanopowders are characterized by the existence of large agglomerates of nanoparticles (NPs), whose size and density determine the fluidizability of the powder. The system studied in this work is a silica nanopowder fluidized in a polycarbonate vessel. We show results from a noninvasive visualization technique able to automatically track NP agglomerate trajectories in the fluidized bed excited by an externally applied alternating field. This technique enables us to measure NP agglomerate properties such as their size, charge, and density. In this work the behavior of a dry-fluidized bed of silica nanopowder as affected by an externally imposed electric field has been studied. Because of contact and tribo charging mechanisms, the NP agglomerates naturally accumulate sufficient electrostatic charge to be appreciably excited by electrostatic fields of strength on the order of 1 kV/cm. A main result from a statistical analysis based on particle tracking velocimetry is that NP agglomerates may carry an electrostatic charge in the fluidized bed up to 100 fC, which is attributable to the large specific surface area of nanopowders and to the high level of charge transfer between silica and the polymeric wall.

INTRODUCTION

Gas bubbles usually developed in gas-fluidized beds of coarse grains (grain size of the order and larger than 100 microns) serve as a bypass for the gas, which hampers the gas-solids contact efficiency. In contrast, gas-fluidized beds of some micron and sub-micron particles exhibit a nonbubbling fluidlike behavior. For example, powders of moderate density NPs, such as silica NPs, can be fluidized by a gas. Fluidization of NPs, providing extremely high specific surface area, has become thus a subject of research interest in the last years. NP fluidization has been successfully applied in processes involving low gas velocities. The use of fluidized beds of titania NPs has been proposed to remove pollutant nitrogen oxides from air by photocatalytic reaction. Fluidization of Co/Al_2O_3 NPs has been shown to be useful to improve the catalytic activity of reforming methane with CO_2. Another example is Atomic Layer Deposition (ALD), which has been successfully carried out in NP fluidized beds to coat NPs with ultra-thin layers of functional. Large-scale processes, involving NP fluidization, currently employed in industry, are the production of fumed metal oxides, such as fumed silica, and carbon black materials. See van Ommen et al. (1) for an extensive recent review on fluidization of nanopowders.

Unfortunately, most nanopowders cannot be uniformly fluidized, thus hampering the efficiency of industry processes relying on the potentially high gas-solids contact surface provided by NPs. Various methods to assist fluidization of nanopowders have been proposed which are useful in either mobilizing or disrupting large and compact agglomerates formed during storage. These

methods include vibration, stirring, sound waves; pulsed flow, centrifugal fields, electric fields, and secondary gas flow from a microjet (van Ommen et al. (1)). In this work we report on the use of a non-invasive direct visualization technique to track NP agglomerate trajectories and measure their size, density, and electrostatic charge.

EXPERIMENTAL SETUP AND PROCEDURE

The nanopowder tested is Aerosil R974 supplied from Evonik Industries, which consists of hydrophobic silica NPs (particle density 2250 kg/m^3 and particle size 12 nm). The nanopowder is pre-sieved (sieve opening of 425 microns) and initialized in the fluidization cell by applying a sufficiently high gas velocity (3 cm/s). The dynamics of NP agglomerates was investigated by automatic tracking NP agglomerates in the vicinity of the free surface. The visualization technique used consisted of laser-based planar imaging as described elsewhere (Wng et al. (2), Valverde et al. (3)). The experimental setup for this purpose is illustrated in Figure 1, where a rectangular polycarbonate bed (4.5x 2.5 cm^2 cross-section). Agglomerate size was directly obtained by means of digital image analysis while agglomerate charge and density were obtained by fitting the experimental trajectories to the trajectories theoretically predicted for a uniformly charged sphere of diameter equal to the measured agglomerate size.

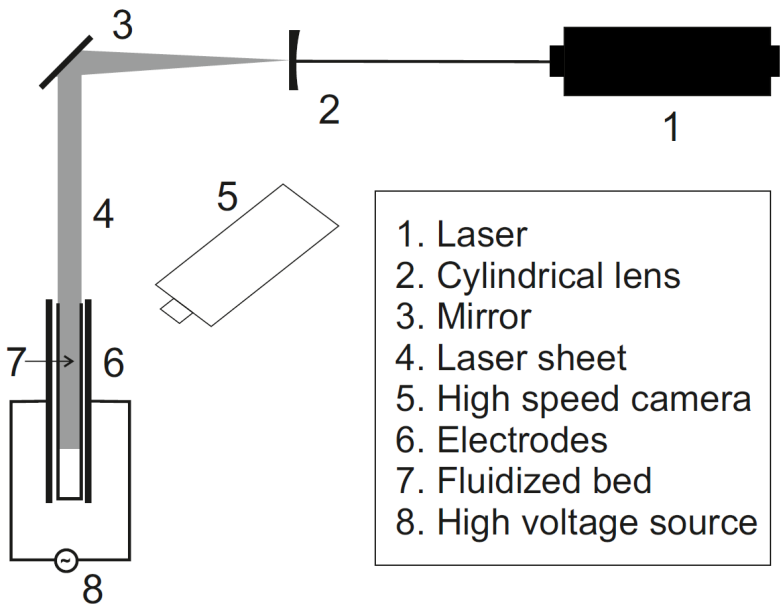

Figure 1: Layout of the experimental setup for NP agglomerate tracking.

EXPERIMENTAL RESULTS AND DISCUSSION

The dynamic evolution of a sphere undergoing a horizontal oscillatory motion in a fluid is analytically described in (Landau and Lifshitz (4)). Accordingly, the trajectory of a sphere charged with an electrical charge Q and subjected to an alternating horizontal electric field will be given by

$$\vec{r}(t) = v\cos(\omega t + \varphi)\,\vec{u}_x \qquad (1)$$

where

$$v = \frac{QE}{6\pi\eta R}\left(\left(1+\frac{R}{\delta}\right)^2 + \left(R\sqrt{\frac{\rho\omega}{2\eta}}\left(1+\frac{2R}{9\delta}\right)\right)^2\right)^{-1/2}$$

$$\delta = \sqrt{\frac{\eta}{\rho\omega}}$$

Here $\omega = 2\pi f$, t is time, φ is the initial phase, $\vec{u}_x$ is the unit vector in the horizontal direction, E is the field strength, R is the sphere radius, $\eta = 1.8\cdot10^{-5}\ \mathrm{Pa\cdot s}$ is the gas viscosity, and $\rho = 1.2\ \mathrm{kg/m^3}$ is the gas density.

In our case, NP agglomerates suspended in the gas flow can be ideally considered as effective spheres oscillating in the gas due to the alternating electric force. Accordingly, the theoretical trajectory of a single agglomerate of radius R and charge Q as a function of time t would be described by Eq. 1. This equation could be simplified in the limit $R/\delta \to 0$, in which the Stokes law for the drag force $F_D = 6\pi\eta R v$ would be valid. However, it is important to remark that this simplification is not valid in our case since $R \not\ll \delta$ in the range of frequencies tested. Thus, the equation for the drag used to derive Eq. 1 is $F_D = 6\pi\eta R\,(1+R/\delta)\,v + 3\pi R^2\sqrt{2\,\eta\,\rho/\omega}\,(1+2R/9\delta)\,dv/dt$.

Images of the fluidized bed close to the free surface, where agglomerate concentration is small, were acquired at 462 frames per second. Figure 2a shows a snapshot of the NP agglomerates captured by means of a CMOS high-speed camera. In Figure 2b trajectories of NP agglomerates as calculated by the tracking software are shown. These trajectories were automatically captured by the image software thus allowing us to perform a robust statistical analysis. Figure 3 is an example of an agglomerate tracked trajectory. The oscillatory trajectory is well fitted by Eq. 1 (the initial drift of the agglomerate has to be added to Eq. 1) using the charge as the only fitting parameter, which serves us to have an estimation of the agglomerate charge. The size of the agglomerates was directly computed by means of the image analysis software.

Results of the distribution of agglomerate radius obtained in this way are displayed in Fig. 4. The average measured size for agglomerates in our experiments (around 200 μm) is similar to the reported in the literature from other techniques as reviewed in van Ommen et al. (1).

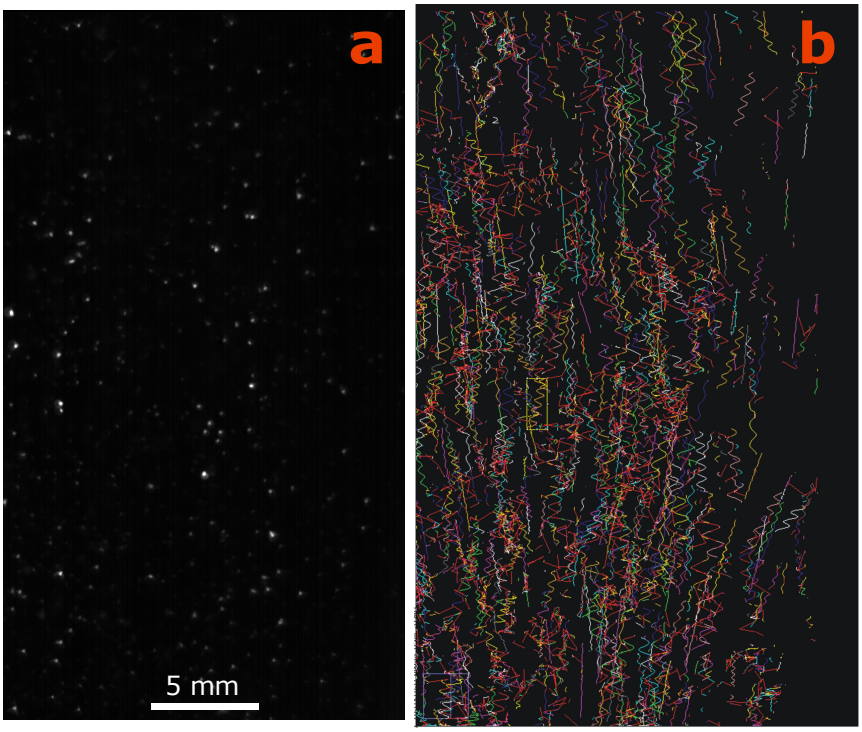

Figure 2: a) Snapshot of NP agglomerates close to the free surface of the fluidized bed (f=50 Hz, E=2.4 kV/cm, v_g=3.2 cm/s). The resolution of the image is 32.55 mm/pixel. b) Trajectories of agglomerates detected in a series of frames within a time lag of 108 ms. Frame rate is 462 frames per second.

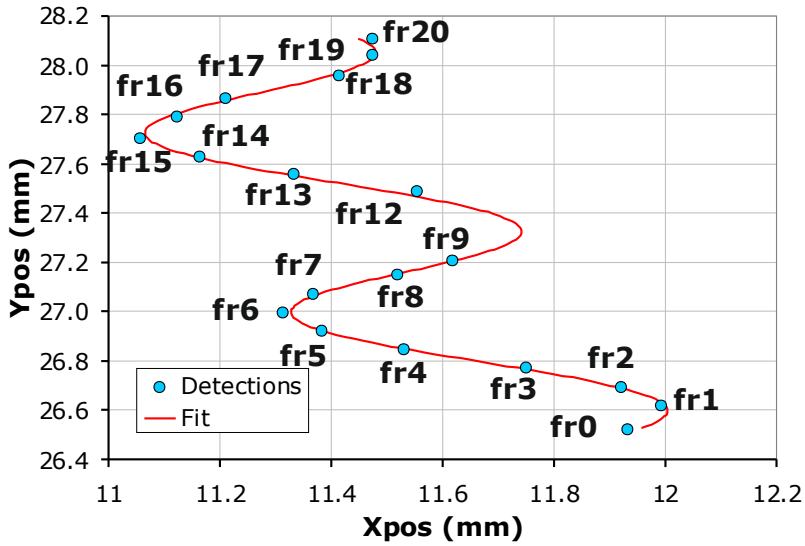

Figure 3: Example of an automatically tracked agglomerate trajectory. The dots mark measured positions of the agglomerate at successive frames (fr). The red line is the fitted theoretical trajectory using the charge in Eq. 1 as fitting parameter and adding the initial drift.

Results of the agglomerate charge obtained by fitting the experimental agglomerate trajectory to the theoretically predicted are shown in Fig. 5. As can be seen, the charge of the agglomerates automatically tracked turns to be mostly between 10 and 100 fC. According to our statistical results, and if agglomerates are approximated by smooth spheres, their surface charge density would be approximately constant and around 1 $\mu C/m^2$ as seen in Fig. 6.

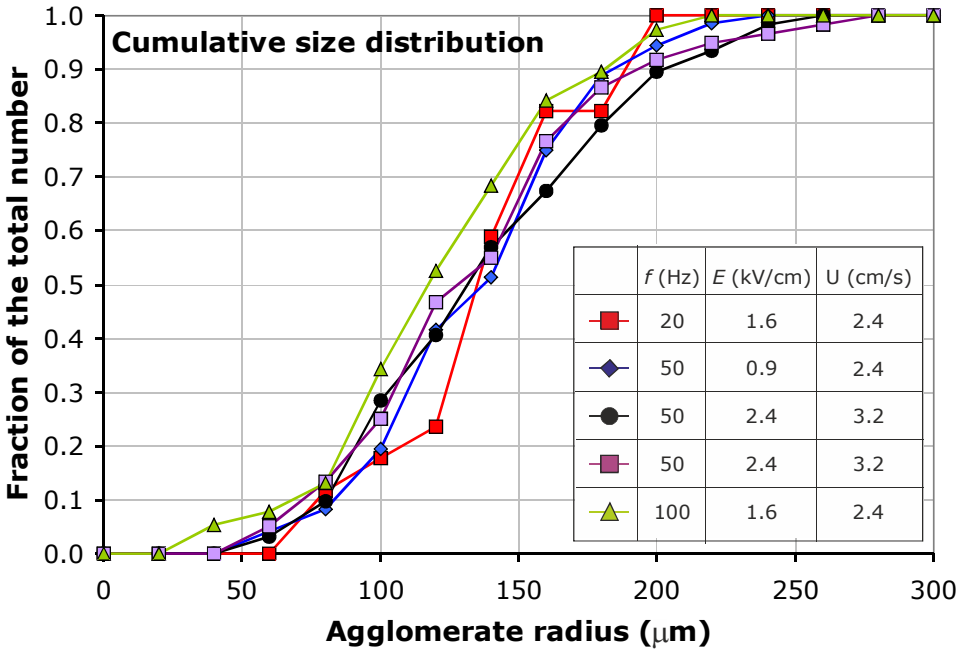

Figure 4: Agglomerate size distribution measured for the different values of the field frequency f, field strength E and superficial gas velocities.

An interesting observation in our experiments was that the velocity of the NP agglomerates was increased after they became in contact with the cell walls. This suggests that the main charging mechanism of these agglomerates is contact charging between the silica NPs and the polycarbonate cell walls. When two insulators with different dielectric constants are in contact, it is energetically favorable that the one with the higher dielectric constant (silica in our case: $\varepsilon_r \approx 4$) donates electrons to the one with lower dielectric constant (polycarbonate in our case: $\varepsilon_r \approx 2-3$) as inferred from the correlation between the order of materials in the triboelectric series and their dielectric constant (Gallo and Lama (5)). However, according to the agglomerate trajectories observed in our experiment, silica NP agglomerates had charge of different sign, which suggests that other effects such as particle size effects play a role on contact charging during collisions.

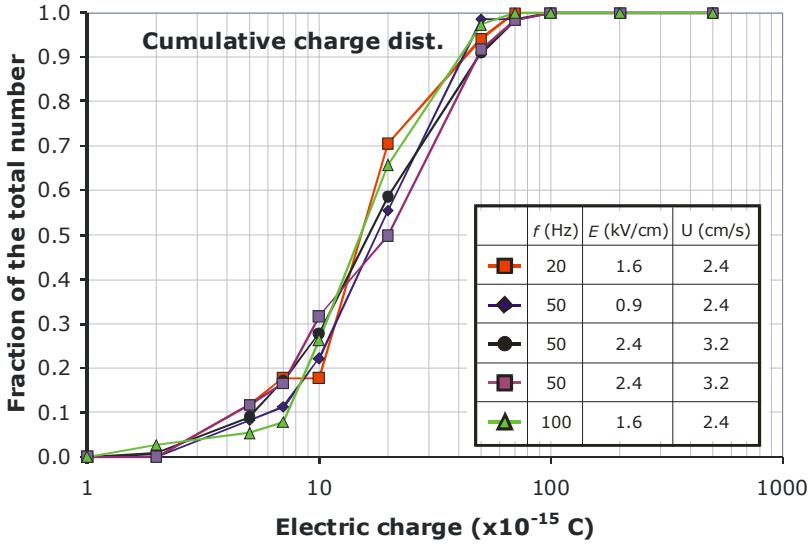

Figure 5: Agglomerate electric charge distribution measured for different values of the field frequency f, field strength E and superficial gas velocities.

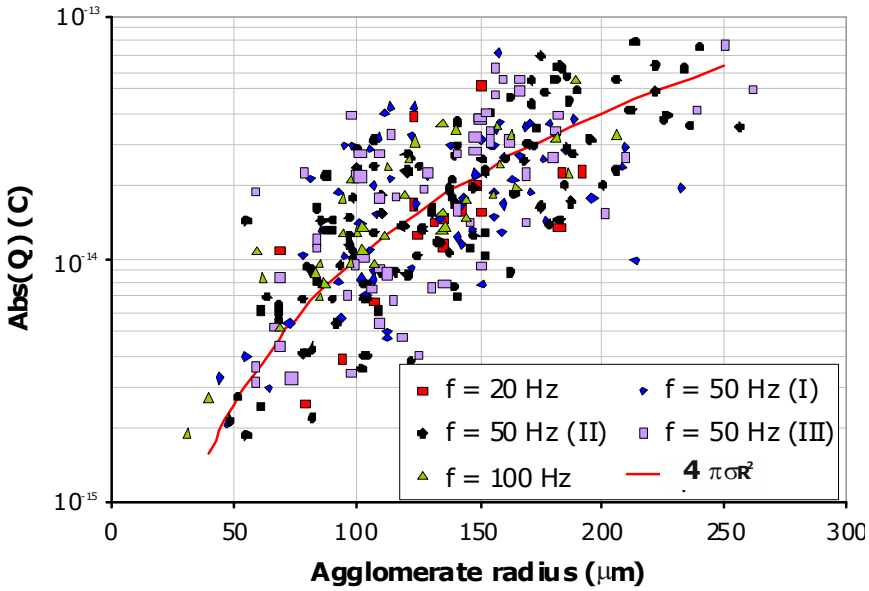

Figure 6: Agglomerate charge vs. size distributions. The red line represents the charge-size distribution for spheres with a surface charge density $\sigma = 10^{-6}$ C/m^2.

The vertical component of the velocity of the agglomerates v_z can be approximated to the velocity of a single sphere of radius R subjected to a vertical gas velocity v_g and oscillating in the horizontal direction

$$v_z - v_g = \frac{2}{9}\left(\frac{\rho^* - \rho}{\eta}\right)\frac{g R^2}{1+\frac{R}{\delta}} \qquad (2)$$

where $g = 9.81\ \mathrm{m/s^2}$ is the gravitational acceleration. In this way, the density of the agglomerates ρ^* can be estimated by equating the vertical component of the velocity experimentally measured from the agglomerate tracks to Eq. 2. The results obtained are plotted in Fig. 7 as a function of the agglomerate radius R .

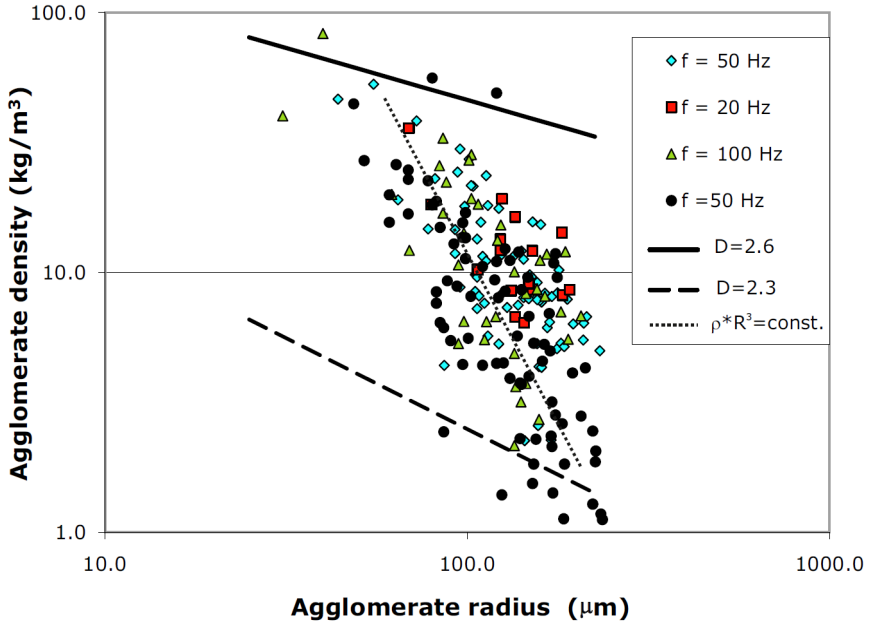

Figure 7: Agglomerate density vs. size distributions. The top and bottom lines represent the expected trends assuming that agglomerates can be characterized by a fractal dimension D=2.3 (dashed line) and D=2.6 (solid line). The dotted line shows that, within the experimental scatter, the agglomerate weight is constant.

We observe that, according to our measurements, the density of the agglomerates analyzed varies between 1 and 100 kg/m^3. Using the fractal model, agglomerate density would be predicted as $\rho^* = \rho_p k^{D-3}$, where ρ_p is the particle density. In Fig. 7 we have plotted the theoretical densities for fractal agglomerates of D=2.3 and D=2.6 as a function of agglomerate radius. As can be seen most of the experimental data are found between these two lines, with the smaller agglomerates close to D=2.6 and the larger ones close to D=2.3. It must be reminded that the agglomerates tracked in the fluidized bed are complex-agglomerates formed by pre-existing simple agglomerates (of size of the order of 10 μm) due to van der Waals force of attraction between them (electrostatic forces between agglomerates are negligible as compared to van der Waals forces as shown in Valverde e tal. (6)). The density of these simple-agglomerates

can be estimated as $\rho_s = \rho^* k_s^{3-D}$, where k_s is the ratio of the complex-agglomerate size to simple-agglomerate size. Using average values, it is $\rho_s \approx 50\ \mathrm{kg/m^3}$. During tapping, these simple-aggregates (formed by aggregation of smaller sub-agglomerates [12]) may be broken and compacted. The tapped density of the nanopowder may thus reach similar values to ρ_s (the typical tapped density reported by Evonik for Aerosil R974 is around $50\ \mathrm{kg/m^3}$, although this value may be subjected to large variations depending on the tapping conditions).

CONCLUSIONS

Because of contact and tribo charging mechanisms, silica NP agglomerates in dry fluidized beds naturally accumulate sufficient electrostatic charge to be appreciably excited by electrostatic fields of strength on the order of 1 kV/cm. A main result from a statistical analysis based on particle tracking velocimetry is that NP agglomerates may carry an electrostatic charge in the fluidized bed up to 100 fC. Measurements of agglomerate size and density in the region close to the free surface indicate that, while the size distribution is wide, the weight of the agglomerates is approximately constant. This suggests that the fluidized bed is mainly stratified by agglomerate weight, with the lightweight agglomerates in the vicinity of the free surface and the heavy agglomerates sinking to the bottom of the bed. Since the electric field strength needed to excite the agglomerates must be larger than their weight, an effective technique to assist fluidization would consist of application of a spatially nonuniform alternating electric field, which is weak in the vicinity of the free surface but strong close to the bottom of the bed.

REFERENCES

[1] Van Ommen, J. R.; Valverde, J. M.; Pfeffer, R. Fluidization of Nanopowders – A Review. J. Nanopart. Res. 2012, 14, 737.

[2] Wang, X. S.; Palero, V.; Soria, J.; Rhodes, M. J. Laser–based planar imaging of nano–particle fluidization: Part I–determination of aggregate size and shape. Chem. Eng. Sci. 2006, 61, 5476–5486.

[3] Valverde, J. M.; Quintanilla, M. A. S.; Castellanos, A.; Lepek, D.; Quevedo, J.; Dave, R. N.; Pfeffer, R. Fluidization of fine and ultrafine particles using nitrogen and neon as fluidizing gases. AIChE J. 2008, 54, 86–103.

[4] Landau, L. D.; Lifshitz, E.M. Fluid Mechanics, Course of Theoretical Physics Vol. 6; Pergamon Press: New York, 1995.

[5] Gallo, C. F.; Lama, W. L. Some charge exchange phenomena explained by a classical model of the work function. J. Electrostat. 1976, 2, 145–150.

[6] Valverde, J. M.; Quintanilla, M. A. S.; Espin, M. J.; Castellanos. A. Nanofluidization Electrostatics. Phys. Rev. E. 2008, 77, 031301.

ACKNOWLEDGEMENTS

This work was supported by the Andalusian Government (Junta de Andalucia, contract FQM-5735) and Spanish Government Agency Ministerio de Ciencia y Tecnologia (contract FIS2011-25161).